IL NUOVO CIMENTO Vol. 33 C, N. 2 Marzo-Aprile 2010
DOI 10.1393/ncc/i2010-10604-3

Colloquia: LC09

The quest for dark matter with the Fermi experiment

A. Morselli
INFN, Sezione di Roma Tor Vergata - Rome, Italy

(ricevuto il 17 Febbraio 2010; approvato il 25 Marzo 2010; pubblicato online il 18 Giugno 2010)

Summary. — The Fermi Large Area Telescope is providing the measurement of the high energy (20 GeV to 1 TeV) cosmic-ray electrons and positrons spectrum with unprecedented accuracy. This measurement represents a unique probe for studying the origin and diffusive propagation of cosmic rays as well as for looking for possible evidences of dark matter. In this framework, we discuss possible interpretations of Fermi results in relation with other recent experimental data on energetic electrons and positrons and in the searches of gamma-ray fluxes coming from WIMP pair annihilations in the sky.

PACS 96.50.sb – Composition, energy spectra and interactions.
PACS 95.35.+d – Dark matter (stellar, interstellar, galactic, and cosmological).
PACS 95.85.Ry – Neutrino, muon, pion, and other elementary particles; cosmic rays.
PACS 98.70.Sa – Cosmic rays (including sources, origin, acceleration, and interactions).

1. – Description

Recently the experimental information available on the Cosmic Ray Electron (CRE) spectrum has been dramatically expanded as the Fermi-LAT Collaboration [1, 2] has reported a high-precision measurement of the electron spectrum from 20 GeV to 1 TeV performed with its Large Area Telescope (LAT) [3]. The spectrum shows no prominent spectral features and it is significantly harder than that inferred from several previous experiments. These data together with the PAMELA data on the rise above 10 GeV of the positron fraction [4] are quite difficult to explain with just secondary production [5-7]. The temptation to claim the discovery of dark matter is strong but there are competing astrophysical sources, such as pulsars, that can give strong flux of primary positrons and electrons (see [8-11] and references therein). At energies between 100 GeV and 1 TeV the electron flux reaching the Earth may be the sum of an almost homogeneous and isotropic component produced by Galactic supernova remnants and the local contribution of a few pulsars with the latter expected to contribute more and more significantly as the energy increases.

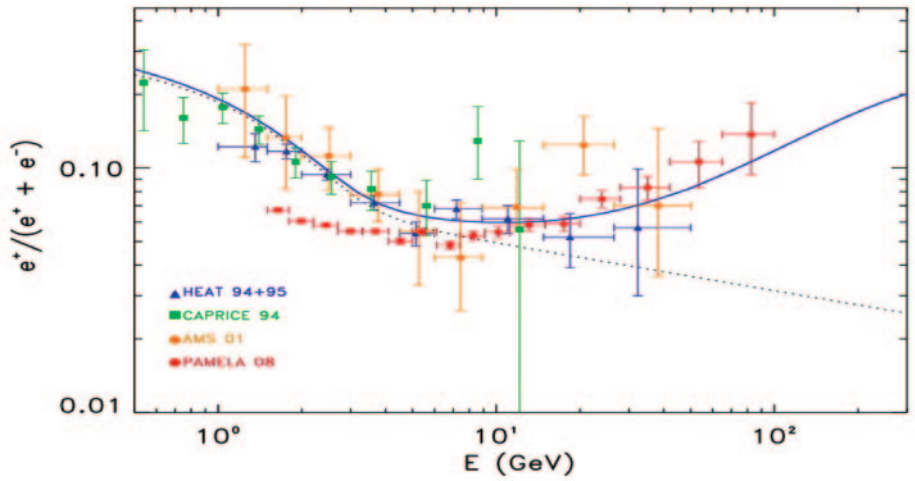

Fig. 1. – PAMELA data and a possible contribution from Monogem and Geminga pulsars [11]. Black-dotted line shows the background from secondary positrons in cosmic rays from GALPROP.

Two pulsars, Monogem, at a distance of $d = 290\,\mathrm{pc}$ and Geminga, at a distance of $d = 160\,\mathrm{pc}$, can give a significant contribution to the high energy electron and positron flux reaching the Earth and with a set of reasonable parameters of the model of electron production we can have a nice fit of the PAMELA positron fraction [4] and Fermi data (see figs. 1 and 2), but it is true that we have a lot of freedom in the choice of these parameters because we still do not know much about these processes, so further study on high energy emission from pulsars is needed in order to confirm or reject the pulsar hypothesis.

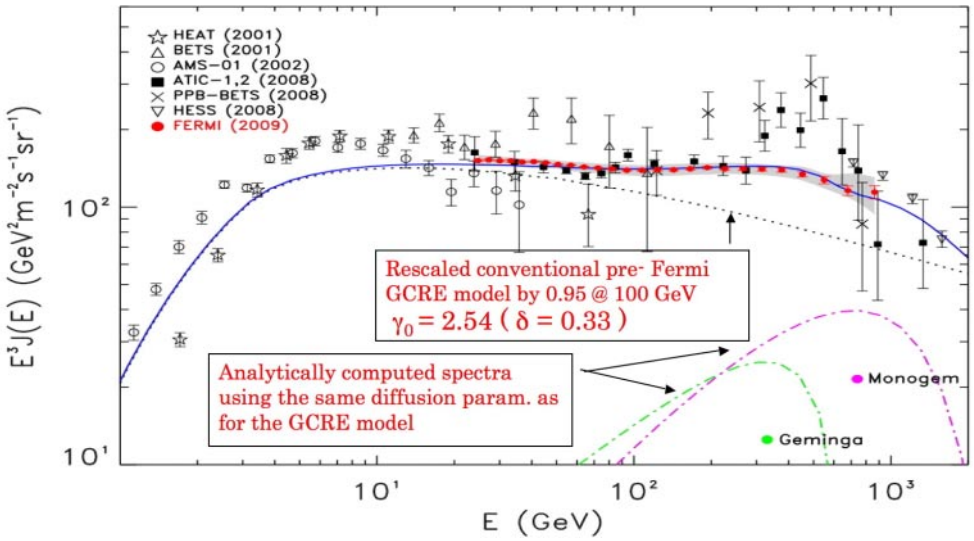

Fig. 2. – (Colour on-line) Electron-plus-positron spectrum (blue continuous line) for the same scenario as in fig. 1. The gray band represents systematic errors on the Fermi-LATdata [3].

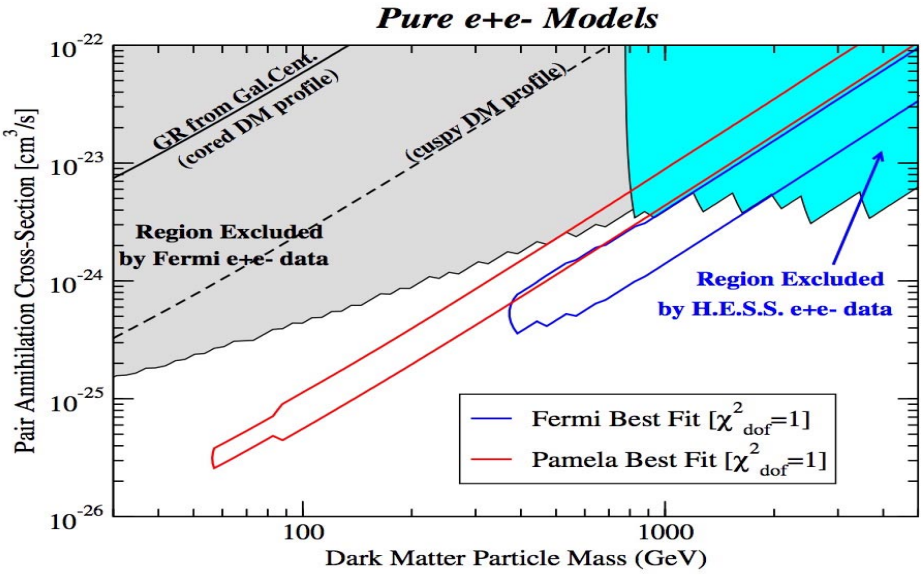

Fig. 3. – (Colour on-line) The parameter space of particle dark matter mass *vs.* pair-annihilation rate, for models where dark matter annihilates into monochromatic $e^{\pm}$. Models inside the regions shaded in gray and cyan over-produce $e^{\pm}$ from dark matter annihilation with respect to the Fermi-LAT and H.E.S.S. measurements, at the 2-σ level. The red and blue contours outline the regions where the χ^2 per degree of freedom for fits to the PAMELA and Fermi-LAT data is at or below 1.

Nevertheless a dark-matter interpretation of the Fermi-LAT and of the PAMELA data is still an open possibility. In fig. 3 we show the parameter space of particle dark matter mass *vs.* pair-annihilation rate, for models where dark matter annihilates into monochromatic $e^{\pm}$ [11]. The preferred range for the dark matter mass lies between 400 GeV and 1–2 TeV, with larger masses increasingly constrained by the H.E.S.S. results. The required annihilation rates, when employing the dark matter density profile imply typical boost factors ranging between 20 and 100, when compared to the value $\langle \sigma v \rangle \sim 3 \times 10^{-26}\,\mathrm{cm}^3/\mathrm{s}$ expected for a thermally produced dark matter particle relic.

How can one distinguish between the contributions of pulsars and dark matter annihilations? Most likely, a confirmation of the dark matter signal will require a consistency between different experiments and new measurements of the reported excesses with large statistics. The observed excess in the positron fraction should be consistent with corresponding signals in absolute positron and electron fluxes in the PAMELA data and all lepton data collected by Fermi. Fermi has a large effective area and long projected lifetime, 5 years nominal with a goal 10 years mission, which makes it an excellent detector of cosmic-ray electrons up to ~ 1 TeV. Future Fermi measurements of the total lepton flux with large statistics will be able to distinguish a gradual change in slope with a sharp cutoff with high confidence [12]. The latter can be an indication in favor of the dark matter hypothesis. A strong leptonic signal should be accompanied by a boost in the γ-ray yield providing a distinct spectral signature detectable by Fermi.

The Galactic Center (GC) is expected to be the strongest source of γ-rays from DM annihilation, due to its coincidence with the cusped part of the DM halo density

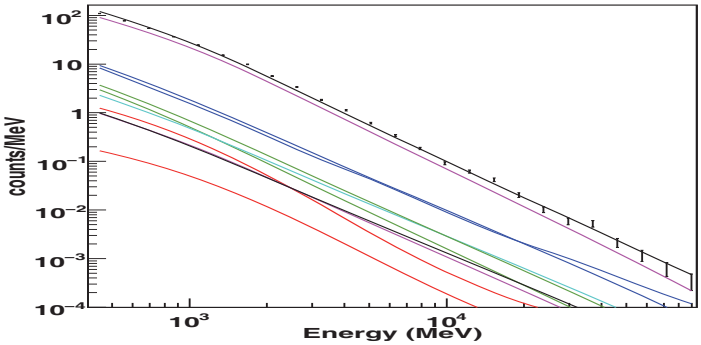

Fig. 4. – (Colour on-line) Spectra from the likelihood analysis of the Fermi/LAT data (number of counts *vs.* reconstructed energy) in a $7° \times 7°$ region around the Galactic Center (number of counts *vs.* reconstructed energy). The likelihood analysis is the standard one used with the LAT data. The main analysis steps are: 1) to select data of high quality (selection cuts on events energy, zenith angle, reconstruction and classification quality); 2) to build an emission model of the region, based on the previous knowledge and experimental evidence of new excesses with enough statistical significance; 3) to apply the likelihood analysis to the data and the considered model. For each model component a fit of the free parameters and the computation of the statistical significance is obtained. Here in the plot, from above to below: the black points are the observed data; the black line is the sum of all the components; the pink line is the Galactic diffuse emission; the lower black line is the isotropic extragalactic; the other components are the sources detected. These results are preliminary.

profile [13, 14]. A preliminary analysis of the data, taken during the first 11 months of the Fermi satellite operations, is shown in figs. 4 and 5.

The reported results were obtained with a binned likelihood analysis, performed by means of the tools developed by the Fermi/LAT Collaboration (gtlike, from the Fermi analysis tools [15]). For this analysis:

– a ROI of $7° \times 7°$ was considered. This ROI was used in order to minimize the background contribution and to avoid significative leakage of the gamma-ray signal under study.

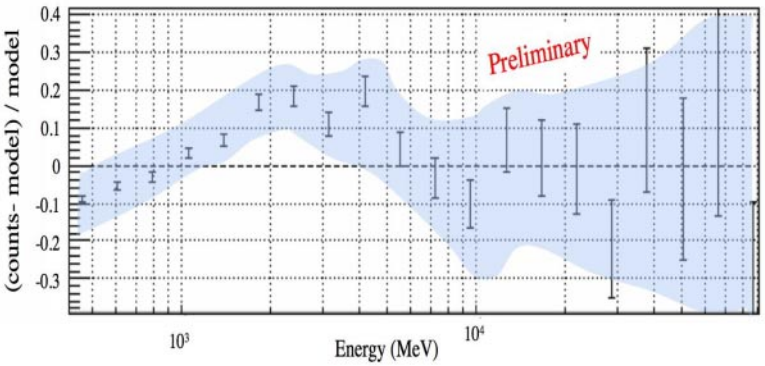

Fig. 5. – (Colour on-line) Residuals ((exp.data - model)/model) of the above likelihood analysis. The blue area shows the systematic errors on the effective area. These results are preliminary.

– The ROI was centred at the position RA = 266.46°, Dec = −28.97°, *i.e.* the position of the brightest source.

– The data taken during the first 11 months (8/2008-7/2009) have been used.

– The events were selected to have energy between 400 MeV and 100 GeV.

– Only events classified of "diffuse" class were and which converted in the *front* part of the tracker have been selected for the analysis. The selection in energy, event classification and conversion provided us with events with very well reconstructed incoming direction and data have been binned into a 100×100 bins map.

– The IRF and the events classification are those relative to the Pass6V3 version of the Fermi/LAT analysis software.

In order to perform the likelihood analysis for the LAT data, a model of the already known sources and the diffuse background should be built. The model in use for the presented analysis contains 11 sources in the Fermi 1 year catalog (to be published) which are located into or very close to the considered ROI. These sources have a point-like spatial model and a spectrum in the form of a power law. The model also contains the diffuse gamma-ray background which is made up of two components:

1) the Galactic diffuse gamma-ray background. The observed Galactic Diffuse emission was modelled by means of the GALPROP code [16] and [17], and the realization of the galactic emission named gll_iem_54_87Xexph7S.fit was used. During the likelihood maximization only the normalization of the GALPROP model is varied, not its components;

2) the Isotropic Background. This component should account for both the Extra-galactic gamma-ray emission and residual charged particles. It is modelled as an isotropic emission with a template spectrum.

The diffuse gamma-ray backgrounds and discrete sources, as we know them today, can account for the large majority of the detected gamma-ray emission from the Galactic Center. Nevertheless a residual emission is left, not accounted for by the above models [18].

Improved modelling of the Galactic diffuse model as well as the potential contribution from other astrophysical sources (for instance unresolved point sources) could provide a better description of the data. Analyses are underway to investigate these possibilities.

An excess in gamma-ray should also be seen in the Galactic diffuse spectrum. Figure 6 (left) shows the LAT data averaged over all Galactic longitudes and the latitude range $10° \leq |b| \leq 20°$. The hatched band surrounding the LAT data indicates the systematic uncertainty in the measurement due to the uncertainty in the effective area described above. Also shown on the right are the EGRET data for the same region of sky where one can see that the LAT-measured spectrum is significantly softer than the EGRET measurement [19]. Figure 6 (right) compares the LAT spectrum with the spectra of an *a priori* diffuse Galactic emission (DGE) model. While the LAT spectral shape is consistent with the DGE model used in this paper, the overall model emission is too low thus giving rise to a $\sim$ 10–15% excess over the energy range 100 MeV to 10 GeV. However, the DGE model is based on pre Fermi data and knowledge of the DGE. The difference between the model and data is of the same order as the uncertainty in the measured CR nuclei spectra at the relevant energies. Overall, the agreement between

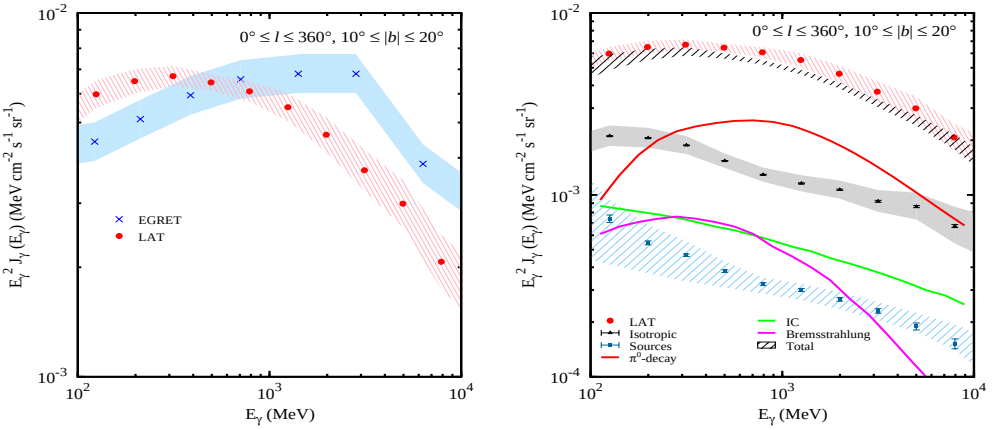

Fig. 6. – (Colour on-line) Left: preliminary diffuse emission intensity averaged over all Galactic longitudes for latitude range $10^\circ \leq |b| \leq 20^\circ$. Data points: Fermi LAT, red dots; EGRET, blue crosses. Systematic uncertainties: Fermi LAT, red; EGRET, blue. Right: preliminary Fermi LAT data with model, source, and isotropic components for the same sky region.

the LAT-measured spectrum and the model shows that the fundamental processes are consistent with our data, thus providing a solid basis for future work understanding the DGE.

Also at higher latitudes for the moment we did not observe any excess. In fig. 7 we show the diffuse γ-rays in a mid-latitude region in the third quadrant (Galactic longitude

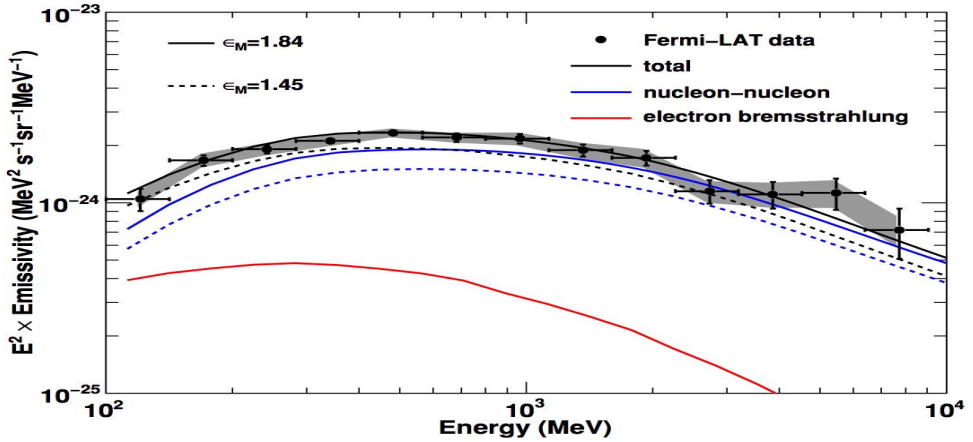

Fig. 7. – Differential γ-ray emissivity from the local atomic hydrogen gas compared with the calculated γ-ray production. The horizontal and vertical error bars indicate the energy ranges and 1 σ statistical errors, respectively. Estimated systematic errors of the LAT data are indicated by the shaded area. A nucleus enhancement factor $\epsilon_{\rm M}$ of 1.84 is assumed for the calculation of the γ-rays from nucleon-nucleon interactions. Dotted lines indicate the emissivities for the case of $\epsilon_{\rm M} = 1.45$, the lowest values in the referenced literature.

TABLE I. – *Flux (in* $10^{-9}\,\mathrm{cm}^{-2}\mathrm{s}^{-1}$*), annihilation cross-section upper limits, and decay lifetime lower limits: γ-ray energies measured and corresponding* 95% *c.l. upper limits (CLUL) on fluxes, for* $|b| > 10^\circ$ *plus a* $20^\circ \times 20^\circ$ *square around the Galactic center. For each energy and flux limit,* $\langle\sigma v\rangle_{\gamma\gamma}$ *and* $\langle\sigma v\rangle_{\gamma Z}$ *upper limits, and* $\tau_{\gamma\gamma}$ *and* $\tau_{\gamma Z}$ *lower limits are given for three Galactic dark matter distributions (see text). The systematic error in the absolute energy of the LAT discussed in the text propagates to a* $-20\% + 10\%$ *systematic error on* $\langle\sigma v\rangle_{\gamma\gamma}$*, while for the decay lower limits the systematic error in the absolute energy of the LAT discussed in the text propagates to a* $+10\% - 5\%$ *systematic error on* $\tau_{\gamma\gamma}$*.*

E_γ (GeV)	95%CLUL	$\langle\sigma v\rangle_{\gamma\gamma}$ [γZ] ($10^{-27}\,\mathrm{cm}^3\mathrm{s}^{-1}$)			$\tau_{\gamma\gamma}$ [γZ] (10^{28} s)		
		NFW	Einasto	Isothermal	NFW	Einasto	Isothermal
30	3.5	0.3 [2.6]	0.2 [1.9]	0.5 [4.5]	17.6 [4.2]	17.8 [4.2]	17.5 [4.2]
40	4.5	0.7 [4.2]	0.5 [3.0]	1.2 [7.2]	10.1 [2.9]	10.3 [2.9]	10.0 [2.9]
50	2.4	0.6 [2.7]	0.4 [1.9]	1.0 [4.6]	15.5 [5.0]	15.7 [5.1]	15.4 [5.0]
60	3.1	1.1 [4.2]	0.8 [3.0]	1.8 [7.3]	9.8 [3.5]	10.0 [3.5]	9.7 [3.5]
70	1.2	0.6 [2.0]	0.4 [1.4]	1.0 [3.4]	21.6 [8.2]	21.9 [8.3]	21.5 [8.1]
80	0.9	0.5 [1.7]	0.4 [1.2]	0.9 [2.9]	26.0 [10.4]	26.4 [10.5]	25.8 [10.3]
90	2.6	2.0 [6.0]	1.5 [4.3]	3.5 [10.3]	7.7 [3.2]	7.8 [3.2]	7.6 [3.1]
100	1.4	1.4 [3.8]	1.0 [2.8]	2.4 [6.6]	12.6 [5.4]	12.8 [5.4]	12.5 [5.3]
110	0.9	1.0 [2.7]	0.7 [1.9]	1.7 [4.6]	18.9 [8.2]	19.2 [8.3]	18.8 [8.2]
120	1.1	1.6 [4.0]	1.1 [2.9]	2.7 [6.9]	13.3 [5.9]	13.5 [6.0]	13.2 [5.9]
130	1.8	3.0 [7.3]	2.1 [5.3]	5.1 [12.6]	7.6 [3.4]	7.8 [3.5]	7.6 [3.4]
140	1.9	3.5 [8.4]	2.5 [6.0]	6.0 [14.3]	7.0 [3.2]	7.1 [3.3]	7.0 [3.2]
150	1.6	3.5 [8.2]	2.5 [5.9]	6.0 [14.1]	7.5 [3.5]	7.6 [3.5]	7.4 [3.4]
160	1.1	2.7 [6.3]	2.0 [4.5]	4.7 [10.9]	10.2 [4.8]	10.4 [4.8]	10.1 [4.7]
170	0.6	1.7 [4.0]	1.3 [2.9]	3.0 [6.8]	17.0 [8.0]	17.2 [8.1]	16.9 [7.9]
180	0.9	2.7 [6.1]	1.9 [4.4]	4.6 [10.4]	11.6 [5.5]	11.8 [5.6]	11.6 [5.4]
190	0.9	3.2 [7.1]	2.3 [5.1]	5.5 [12.2]	10.4 [4.9]	10.5 [5.0]	10.3 [4.9]
200	0.9	3.3 [7.3]	2.4 [5.2]	5.7 [12.5]	10.6 [5.1]	10.8 [5.1]	10.5 [5.0]

l from 200° to 260° and latitude $|b|$ from 22° to 60°). The region contains no known large molecular cloud and most of the atomic hydrogen is within 1 kpc of the solar system. The contributions of γ-ray point sources and inverse Compton scattering are estimated and subtracted. The residual γ-ray intensity exhibits a linear correlation with the atomic gas column density in energy from 100 MeV to 10 GeV. The differential emissivity from 100 MeV to 10 GeV agrees with calculations based on cosmic-ray spectra consistent with those directly measured, at the 10% level. The results obtained indicate that cosmic ray nuclei spectra within 1 kpc from the solar system in regions studied are close to the local interstellar spectra inferred from direct measurements at the Earth within $\sim 10\%$ [20].

Finally a line at the WIMP mass, due to the 2γ production channel, could be observed as a feature in the astrophysical source spectrum [12]. Such an observation is a "smoking gun" for WIMP DM as it is difficult to explain by a process other than WIMP annihilation or decay and the presence of a feature due to annihilation into γZ in addition would be even more convincing.

Up to now however no lines was observed and we obtain γ-ray line flux upper limits in the range $0.6 - 4.5 \times 10^{-9}\,\mathrm{cm}^{-2}\mathrm{s}^{-1}$, and give corresponding DM annihilation cross-section and decay lifetime limits shown in table I [21].

2. – Conclusion

Recent accurate measurements of cosmic-ray positrons and electrons by PAMELA, and Fermi have opened a new era in particle astrophysics. The CRE spectrum measured by Fermi-LAT is significantly harder than previously thought on the basis of previous data. Adopting the presence of an extra $e^{\pm}$ primary component with ~ 2.4 spectral index and $E_{\rm cut} \sim 1\,\text{TeV}$ allows to consistently interpret Fermi-LAT CRE data (improving the fit), HESS and PAMELA. Such extra-component can be originated by pulsars for a reasonable choice of relevant parameters or by annihilating dark matter for model with $M_{DM} \sim 1\,\text{TeV}$. Improved analysis and complementary observations (CRE anisotropy, spectrum and angular distribution of diffuse γ, DM sources search in γ) are required to possibly discriminate the right scenario. Their exotic origin has to be confirmed by complimentary findings in γ-rays by Fermi and atmospheric Cherenkov telescopes, and by LHC in the debris of high-energy proton destructions. A positive answer will be a major breakthrough and will change our understanding of the universe forever. On the other hand, if it happens to be a conventional astrophysical source of cosmic rays, it will mean a direct detection of particles accelerated at an astronomical source, again a major breakthrough. In this case we will learn a whole lot about our local Galactic environment. However, independently of the origin of these excesses, exotic or conventional, we can expect very exciting several years ahead of us.

REFERENCES

[1] Atwood W. B. *et al.* (Fermi Collaboration), *Astrophys. J.*, **697** (2009) 1071 [arXiv:0902.1089].
[2] Abdo A. A. *et al.* (Fermi Collaboration), *Astropart. Phys.*, **32** (2009) 193 [arXiv:0904.2226]
[3] Abdo A. A. *et al.* (Fermi Collaboration), *Phys. Rev. Lett.*, **102** (2009) 181101 [arXiv:0905.0025].
[4] Adriani O. *et al.* (PAMELA Collaboration), *Nature*, **458** (2009) 607 [arxiv:0810.4995].
[5] Strong A. W. and Moskalenko I. V., *Astrophys. J.*, **509** (1998) 212; **493** (1998) 694.
[6] Lionetto A., Morselli A. and Zdravkovic V., *JCAP*, **09** (2005) 010 [astro-ph/0502406]; Ptuskin V. S. *et al.*, *Astrophys. J.*, **642** (2006) 902.
[7] Morselli A. and Moskalenko I., *PoS* (idm2008)025 [arXiv:0811.3526].
[8] Boulares A., *Astrophys. J.*, **342** (1989) 807.
[9] Aharonian F. A., Atoyan A. M. and Völk H. J., *Astron. Astrophys.*, **294** (1995) L41.
[10] Coutu S. *et al.*, *Astropart. Phys.*, **11** (1999) 429.
[11] Grasso D. *et al.*, *Astropart. Phys.*, **32** (2009) 140 [arXiv:0905.0636].
[12] Baltz E. *et al.*, *JCAP*, **07** (2008) 013 [arXiv:0806.2911].
[13] Morselli A. *et al.*, *Nucl. Phys. B*, **113** (2002) 213.
[14] Cesarini A., Fucito F., Lionetto A., Morselli A. and Ullio P., *Astropart. Phys.*, **21** (2004) 267 [astro-ph/0305075].
[15] `http://fermi.gsfc.nasa.gov/ssc/data/analysis/software/`.
[16] Strong A. *et al.*, *Astrophys. J.*, **613** (2004) 962S.
[17] Strong A. *et al.*, *Annu. Rev. Nucl. Part. Sci.*, **57** (2007) 285.
[18] Vitale V. and Morselli A. for the Fermi/LAT Collaboration, *2009 Fermi Symposium* [arXiv:0912.3828].
[19] Abdo A. *et al.* (Fermi Collaboration), *Phys. Rev. Lett.*, **103** (2009) 251101 [arXiv:0912.0973].
[20] Abdo A. A. *et al.* (Fermi Collaboration), *Astrophys. J.*, **703** (2009) 1249 [arXiv:0908.1171].
[21] Abdo A. A. *et al.* (Fermi Collaboration), *Phys. Rev. Lett.*, **104** (2010) 091302 [arXiv:1001.4836].